ACS OMEGA

http://pubs.acs.org/journal/acsodf

Article

Pressure Characteristics and Secondary Ignition Effects of Gas Produced in RDE Using Lignite and Anthracite/CH_4 Fuel

Jing Guo,* Shirong Ge, Ruibo Yang, Jiayu Liang, and Yinan Guo

Cite This: *ACS Omega* 2024, 9, 36421−36433

Read Online

ABSTRACT: This study aims to address the energy efficiency release and environmental impact of coal dust in rotating detonation engines (RDEs) by monitoring the detonation characteristics of lignite and anthracite in methane gas−solid mixtures using high-precision sensor technology. Experimental results indicate that the peak detonation pressure of anthracite is 1.4% higher than that of lignite, and its detonation wave propagation speed is at least 5.5% faster, suggesting that anthracite exhibits more stable and efficient fuel energy release characteristics during detonation. Additionally, the sensor technology enabled detailed recording of pressure fluctuations and gas composition changes during the detonation process, providing accurate data for assessing and controlling emissions of harmful gases such as carbon monoxide and carbon dioxide. These data are crucial for designing more efficient and environmentally friendly coal dust detonation systems, enhancing mine safety and environmental protection. The outcomes of this research not only advance technological progress in the field of energy science but also address efficiency and environmental issues in industrial applications, offering significant support for achieving safer and more sustainable energy production methods.

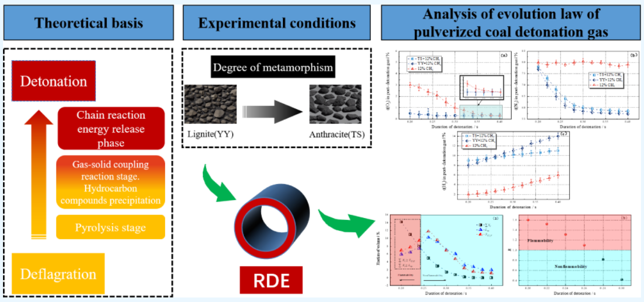

1. INTRODUCTION

Detonation engines have garnered significant attention from researchers over the past few decades due to their high thermal efficiency, simple structure, and high specific impulse.[1,2] Among various types of detonation engines, including pulse detonation engines (PDEs), oblique detonation engines (ODEs), and RDE, the latter has emerged as the most favored by researchers.[3] PDEs operate intermittently and periodically, requiring high-frequency, high-energy ignition, which leads to significant energy losses.[4,5] On the other hand, ODEs typically operate at high Mach numbers and experimental conditions, increasing the cost of associated experimental research.[6,7] In contrast, RDEs offer several advantages, such as singlepoint ignition, continuous operation, self-sustaining and self-compressing detonation waves, effective thrust at low pressure ratios, a wide range of inlet velocities, and a simple structure.[8] These characteristics make RDEs recognized as the most promising combustion devices for the future.

With the rapid development of industry and economy, the demand for efficient energy utilization is becoming increasingly urgent. As a traditional fossil fuel, coal plays an indispensable role in the energy structure. However, the inefficient extraction and high pollution of coal have been a major challenge. Introduced in 2016, the innovative concept of in situ fluidized mining of deep coal integrates various modules, including mining, support, coal sorting, fluidization transformation, and energy storage, into a single conceptual mining apparatus.[9−11] The foundation of this groundbreaking extraction method lies in the detonation combustion of pulverized coal, which aims to transform deep-earth coal resources into alternative energy forms, such as converting fossil fuels into electrical energy, as illustrated in Figure 1. The primary goal is to leverage the RDEs device's ability to efficiently release energy from pulverized coal located deep underground, thus revolutionizing the approach to coal energy utilization.[12,13] Detonation combustion, with its remarkable characteristics, including exceptionally high thermal cycle efficiency, rapid heat release rate, and notably efficient pressure gain, is poised to transform the field of fluidized bed mining for deep coal resources. This technology has the potential to significantly enhance the efficiency and effectiveness of extracting deep coal resources, making it a highly innovative solution for energy acquisition in challenging environments. The distinctive properties of detonation combustion could establish it as a key technological advancement and a crucial option in the pursuit of more

Received: April 25, 2024
Revised: July 31, 2024
Accepted: August 7, 2024
Published: August 13, 2024

https://doi.org/10.1021/acsomega.4c03972
ACS Omega 2024, 9, 36421−36433

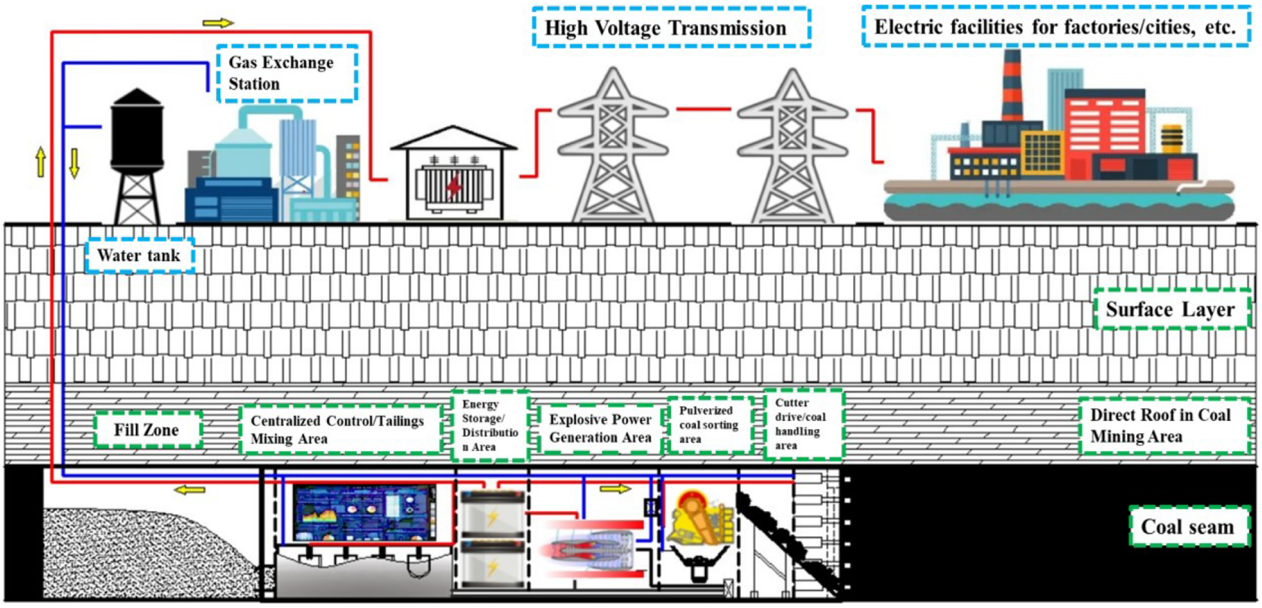

Figure 1. Concept diagram of detonation mechanism system of underground intelligent coal mining.[34]

efficient and sustainable energy production methods in the mining sector.

The concept of rotating detonation was first discovered by Voitsekhovskii from the former Soviet Academy of Sciences in 1959 while investigating transverse detonation waves.[14] By igniting a mixture of argon-diluted C_2H_2/O_2 in a disc-shaped combustion chamber, Voitsekhovskii successfully captured the structure of the rotating detonation wave using a fully compensated schlieren photography technique. Since 2000, significant advancements in fundamental disciplines, such as fluid dynamics and materials mechanics, have catalyzed a surge in research outcomes related to Rotating RDEs. Russia, a forerunner in RDE research, has accumulated a substantial body of knowledge in this field. The Frolov team from the Russian Academy of Sciences conducted extensive experimental research using a pulse wind tunnel on hydrogen–air mixtures for RDEs, confirming the feasibility of achieving stable detonation waves in scramjet engines operating at Mach numbers between 4 and 8. Their studies documented detonation wave speeds of up to 1200 m per second and a maximum thrust of 2200 new-tons.[15,16] Furthermore, GHKN Corporation and Locke-Dyne Inc. have investigated RDREs using methane, ethane, and ethylene with oxygen, testing various flow rates and fuel ratios. High-speed photography revealed the presence of 5–8 detonation waves in the chamber, reaching 60–72% of the theoretical Chapman–Jouguet (C–J) speed. Studies indicate that RDRE's specific impulse might achieve 68–85% of an ideal rocket engine's performance at sea level.[17] It is evident that gaseous and liquid fuels are the primary forms utilized in rotating detonation engines (RDEs), with predominant applications in military and aerospace propulsion technologies.

The advantages of solid fuels in detonation applications have been extensively studied and recognized. Compared to gas and liquid fuels, solid fuels offer higher energy density, stable storage and transportation conditions, and enhanced safety, broadening their application prospects in areas such as combustion detonation engines, particularly in environments requiring long-term storage or use under extreme conditions.[18,19] Coal is one of the main energy sources in the world. As a standard solid fuel, it is widely used in the research field of combustion technology. At present, the experimental research of pulverized coal detonation mainly focuses on the analysis of detonation characteristics and the influence of environmental factors. These analyses typically involve laboratory-scale experiments exploring the detonation properties of coal dust under a variety of conditions, including measurements of detonation pressure, flame propagation velocity, and distribution of explosive products. Ren et al. (2024) investigated the diffusion and explosion processes of solid–liquid–air mixtures, providing crucial data for understanding the physicochemical mechanisms of coal dust explosions. Environmental factors such as temperature, pressure, and humidity also influence coal dust detonations.[20] Wang et al. (2020) examined the explosion characteristics of aluminum powder in different gaseous environ-ments, offering experimental evidence for the behavior of coal dust explosions under diverse environmental conditions.[21] Garan et al. (2023) investigated the detonation characteristics of different coal dust concentrations using RDE and found that the coal dust concentration significantly affects the detonation pressure and temperature.[22] Additionally, Hou et al. (2023) studied the effects of ignition location on the explosion characteristics of methane-air mixtures through semienclosed pipe experiments, revealing that the ignition location significantly influences the detonation pressure waveform and flame propagation speed.[23] In the field of numerical simulation, researchers have utilized numerical methods such as Computational Fluid Dynamics (CFD) to simulate the detonation process of coal dust. For instance, Liang et al. (2023) conducted a numerical analysis on the distribution of combustion products in tunnel methane explosions using GASFLOW-MPI software. They discovered that thermal losses significantly influence the temperature characteristics and distribution patterns of the combustion products.[24] Xu et al. (2021) investigated the impact of cavity width on the attenuation characteristics of gas explosion waves through numerical simulations. Their findings indicate that the cavity width significantly affects the duration and peak

https://doi.org/10.1021/acsomega.4c03972
ACS Omega 2024, 9, 36421–36433

overpressure of the flame.[25] Bykovskii and collaborators[26−30] extensively investigated the continuous detonation of various coals, including anthracite and lignite. Their research findings expanded the range of coal types applicable as fuels in rotating detonation engine (RDE) systems.

The gases produced by coal dust detonations mainly include carbon monoxide (CO) and carbon dioxide (CO_2), which can have adverse effects on the environment and human health. Research on the exhaust products of coal dust detonations mainly focuses on the analysis of exhaust components and safety control measures. Studying these products is crucial for understanding the dynamics of continuous coal dust detonations, assessing their impact on mine safety and worker health, and developing effective environmental protection and detonation control technologies. In the field of exhaust composition analysis, Jia and Zhang (2024) conducted experimental research on the minimum ignition temperature of two-phase fuel clouds and established a predictive model. This provides a theoretical basis for preventing the ignition of fuel clouds during high-energy explosions.[31] Yang et al. (2023) used OpenFOAM for numerical simulations of gas explosions, studying the effects of nonuniform concentration distribution on explosion characteristics, thereby providing a theoretical basis for understanding exhaust components.[32] Cveticanin et al. (2020) analyzed the dynamic behavior during the coal combustion process from a new perspective, indirectly supporting the theoretical foundation for exhaust safety protection.[33] In summary, research on coal dust detonation has achieved a series of important results, but there are still some challenges and unresolved issues. Future studies need to delve deeper into the mechanisms of coal dust detonation, optimize experiments, and enhance research on the environmental impact of detonation exhaust gases. Additionally, attention must be paid to the safety of coal dust detonation in actual industrial applications to ensure efficient energy use and sustainable environmental development.

This research continues our group's series of studies on pulverized coal detonation, utilizing the same experimental platform as previous work.[34] However, it focuses on investigating the effects of solid fuels, primarily coal dust, on detonation phenomena in gas−solid two-phase mixtures within rotating detonation engine (RDE) devices.[35] Detonation experiments were conducted on coal dust/CH_4 two-phase mixtures using two different coal types (lignite and bituminous). Through in-depth analysis of detonation phenomena in gas−solid two-phase fuels, patterns influencing rotating detonation wave (RDW) propagation and detonation gas products were summarized. The findings have significant scientific implications for understanding the detonation combustion characteristics of different threshold coal types in loaded environments.

2. MATERIALS AND METHODS

2.1. Experimental Materials. Proximate analysis data for two types of coal (lignite and anthracite) are shown in Table 1. The proximate analysis was conducted according to the Chinese National Standard GB/T 212-2008 "Proximate analysis of coal", which specifies the methods and procedures for determining moisture, ash, volatile matter, and fixed carbon in coal samples. The analysis was carried out using standard equipment such as drying ovens and muffle furnaces, with precise control of temperature and time to determine the content of each component. Pulverized and screened coal from different coal mines (Tashan Mine and Yanya Mine) in Shanxi, China, coal dust with particle size less than 10 μm was obtained. All dust samples (after 24 h of heat treatment at 60 °C) are collected in clean sample bags in preparation for subsequent detonation tests. As can be seen from Table 1, the difference between TS and YY coal samples is that the latter has a lower volatile content and a higher fixed carbon proportion, which is caused by the degree of coalification and metamorphism of the two coal types. The terms M_{ad}, A_{ad}, V_{ad}, and FC_{ad} in Table 1 represent the air-dried basis moisture, ash, volatile matter, and fixed carbon, respectively. These differences in proximate analysis results indicate that the two coal samples are suitable for comparative experimental studies.

Table 1. Approximate Analysis of Two Coal Samples(wt %)

material source	coal samples	M_{ad}	A_{ad}	V_{ad}	FC_{ad}
anthracite	TS	0.8	8.6	8.1	82.54
lignite	YY	1.1	13.8	37.5	47.6

2.2. Experimental Apparatus. Figure 2 depicts a Schematic diagram of the experimental setup, comprising a custom-built RDE main combustion chamber, fuel supply system, oxidizer supply system, ignition system, and control and data acquisition(DAQ) system. The RDE combustors are comprised of a fuel chamber, methane chamber inlet, and powder inlet. The A−A and B−B sections of Figure 2 shows a sectional view of the RDE combustor, which has a coaxial ring structure with an outer ring diameter of 88 mm, an inner ring diameter of 66 mm, and a combustor length of 1000 mm. During operation, fuel and oxygen are preinjected into the RDE combustor and then enter the RDC through evenly distributed orifices, where they participate in mixing and combustion. The coal powder supply system, mainly consists of methane pipelines, powder storage chambers, piston components, and stepper motor. The fuel supply process is as follows: first, ultrafine coal powder is injected into the storage chamber, then the coal powder is compacted by the stepper motor and piston components. Methane methane is introduced into the storage chamber at a set flow rate, carrying the coal powder into the RDE combustion chamber to complete one fuel injection. Both the oxygen pipeline to the RDE and the hydrogen pipeline to the fluidized bed are equipped with sonic nozzles to achieve stable methane flow rates. During the RDE operation, 4 high-frequency pressure sensors (PS_{1-4}) installed on the detonation tube to monitor the continuous detonation state of lignite coal powder. The pressure sensor used is of PCB-113B26 type, with a response time of less than 0.5us, a sampling frequency of 500 kHz, a sensitivity of 0.7−1.5 V/MPa, and a maximum range of 6.8 MPa. (Reprinted (adapted or reprinted in part) with permission from [[34]]. Copyright [2024/Sci. Rep.] [Guo et al./Sci. Rep.].)

2.3. Experimental Procedure. The experimental process is shown in Figure 3. Two kinds of fuel, pulverized coal/CH_4 and pure gas CH_4, were used in detonation experiment. In the experiment, a high energy igniter (2 kJ) was used for ignition operation, and the continuous detonation time was changed by controlling the fuel supply time. After the dust detonation test, the residue of the sampled gas is analyzed. The ambient temperature of detonation test is 24 °C and the relative humidity is 30.5%.

https://doi.org/10.1021/acsomega.4c03972
ACS Omega 2024, 9, 36421−36433

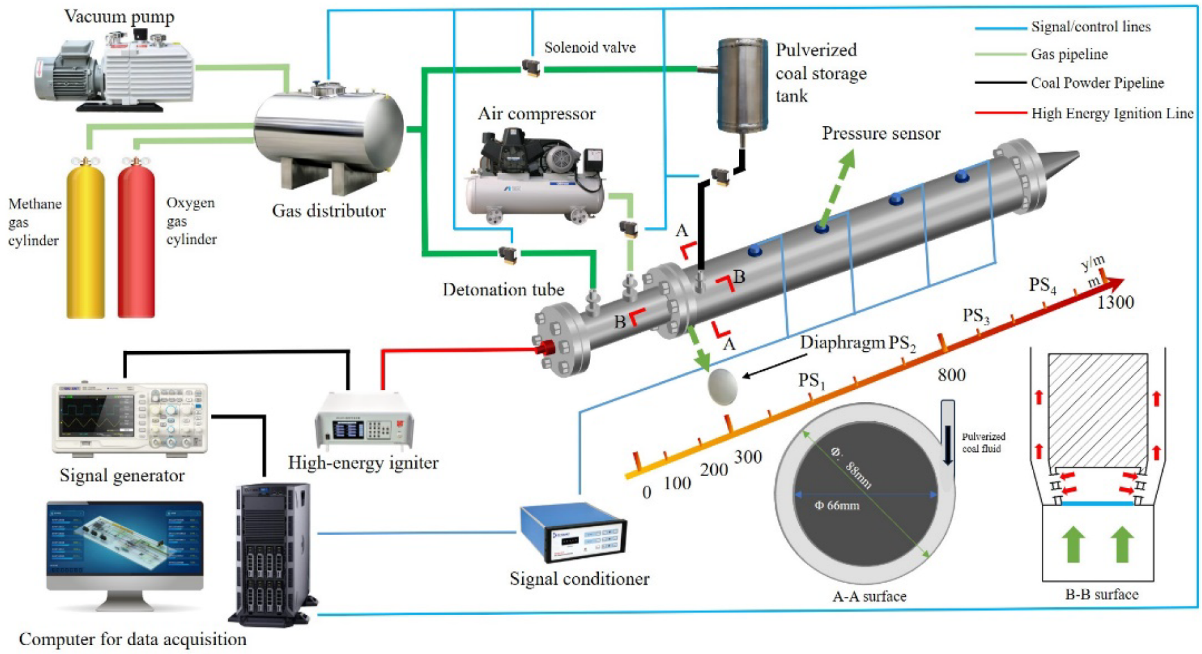

Figure 2. Detonation test equipment.[34]

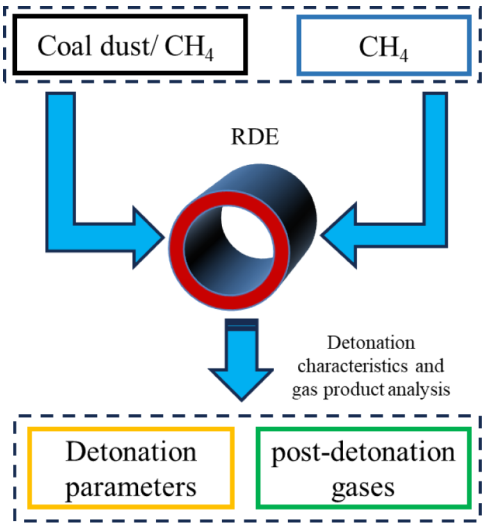

Figure 3. Experimental procedure used in the dust detonation test.

Figure 4 shows the sequential operation time of the self-made RDE using coal/methane fuel. The arrows above the time axis indicate opening, while the arrows below the time axis indicate closing. During the experiment, the coordinated operation of the various parts of the experimental system is achieved by controlling the spark igniter, motor, and various solenoid valves through the control system. A complete engine operation process usually includes fuel preinjection, ignition, RDE combustion chamber operation, and combustion chamber extinguishing. The supply of coal powder fuel requires the transportation of methane. Therefore, before supplying coal powder to the fluidized bed, the stable supply of methane should be ensured. The engine ignition process is completed by preblasting the methane/oxygen mixture through the preblast tube and igniting it with a spark plug. Subsequently, after a certain development time, the coal/methane/oxygen mixture will form a stable nonhomogeneous detonation. To prevent the pressure sensor from being continuously damaged by high temperatures, the experimental duration of the detonation process is preset to Ata = 725 ms. At the end of the experiment, the fuel supply is first cut off. After each test, the RDC was cleaned with high pressure air, and the experiment was repeated three times consecutively to ensure the accuracy of the results of each test scheme. The mean value and standard deviation of the three experimental results were calculated, and the error bar method was used to represent the uncertainty of the measurements. The length of the error bar was taken as 1 standard deviation. This approach improves the reliability of the results by reducing the influence of random errors, quantifies the uncertainty of the measure-

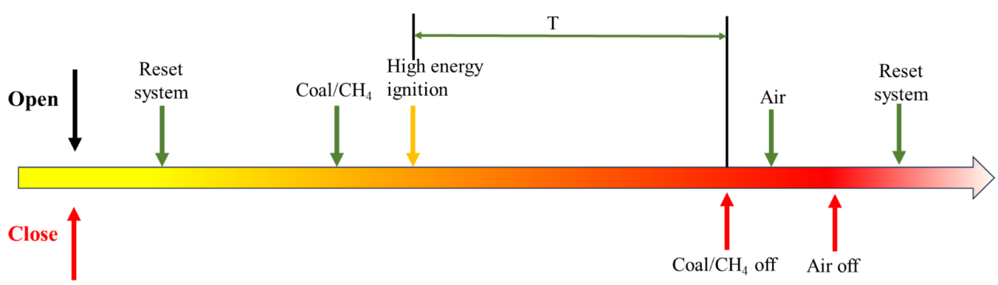

Figure 4. RDE sequential running time.[34]

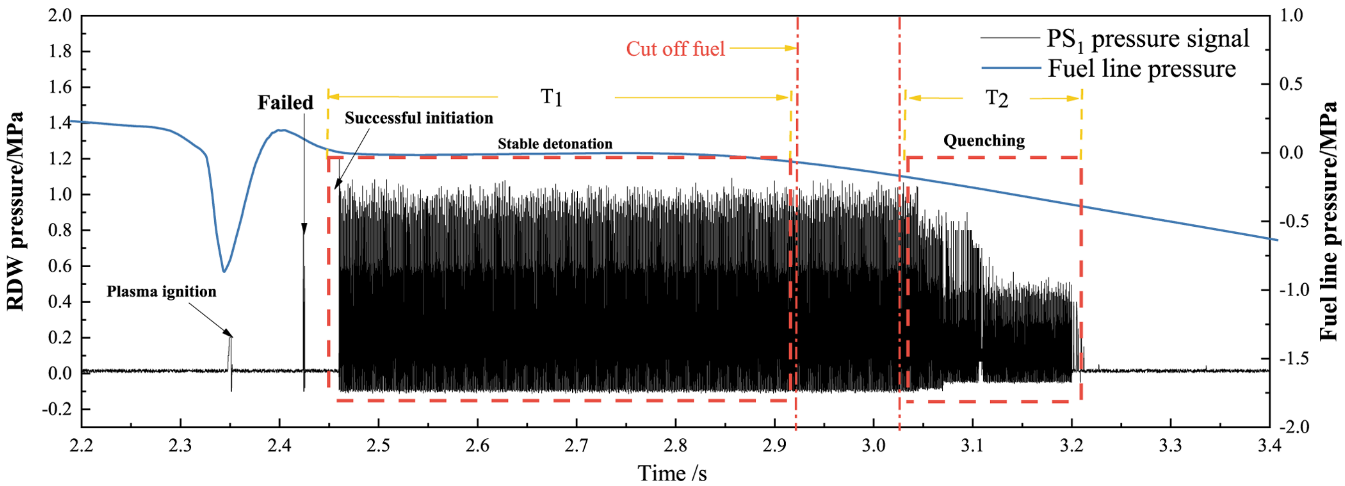

Figure 5. Classic high frequency pressure wave measured by the pressure sensor (Ps_1).

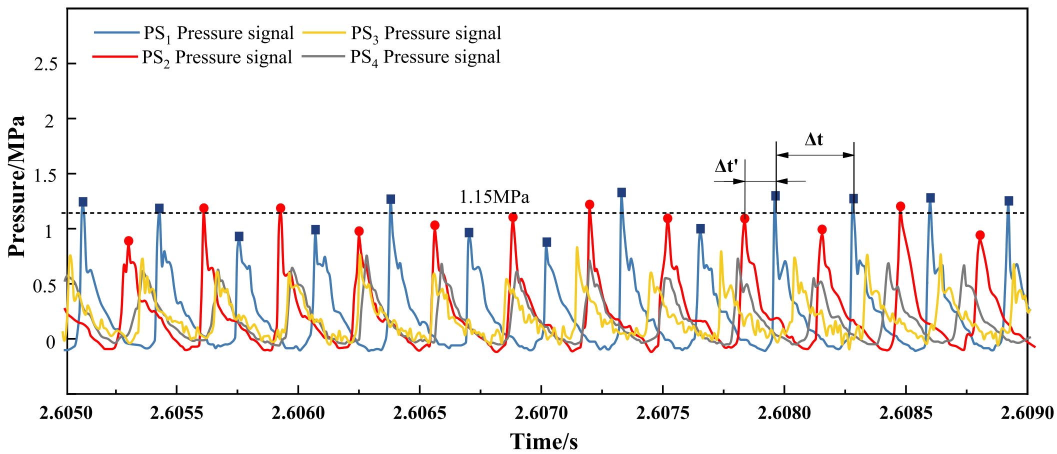

Figure 6. RDW high-frequency pressure signals collected by PS_{1-4}.[34]

ments, and facilitates the comparison and analysis of results between different test schemes, ultimately helping to draw more accurate conclusions.

Different from the deflagging state, continuous detonation is characterized by a stable and sustained pressure wave during detonation. Figure 5 shows the classical high-frequency pressure wave measured by the pressure sensor during a detonation period. It can be seen that when the RDE device reaches a stable state, a pressure wave of about 0.45 s and at least 0.8 MPa can be generated in the detonation tube. However, the pressure wave duration in deflagellation state is often lower than 0.2 s, so this study determined that the detonation state is considered as the detonation state when the measured pressure wave duration is higher than 0.2 s.

For gas analysis, both a Gas chromatograph (GC-9790) and a hydrogen detector (GDX-H_2) were utilized. The composition of the gas chromatograph includes systems for carrier gas, sampling, chromatography, monitoring, along with recording and data analysis. Using an external standard for quantitative analysis, the gas detection achieved a resolution of 1×10^{-6}. The system ensures temperature control accuracy to within ±0.1 °C, with the capability to adjust the temperature from 0.1 to 30 °C per minute. It is important to note that the Gas chromatograph is not designed to measure hydrogen. In contrast, hydrogen detection is carried out by the hydrogen detector through an electrochemical method, also with a resolution of 1×10^{-6}. To confirm the gas analyzer's precision, a gas mixture of specified composition was tested.

3. RESULTS

3.1. Analysis of RDE Detonation Pressure Propagation Characteristics. Figure 6 illustrates the partial pressure curves measured by four sensors PS_{1-4} during the stable propagation phase of the RDW between 2.6050 s and 2.6090 s. The pressure peak recorded by sensor PS_1, positioned closest to the detonation point, is significantly higher compared to the progressively distant sensors PS_2, PS_3, and PS_4. The time difference between adjacent pressure peaks at sensor P_1 is denoted as Δt, while $\Delta t'$ represents the time difference between the peak pressures at PS_1 and PS_2.

It can be found that detonation waves present different propagation characteristics in RDE devices. In this paper, four sensors are proposed to collect pressure wave signals to explore the law of pressure propagation. The state is evaluated based on the signals collected by pressure sensors PS_{1-4} at different positions, and the velocity is calculated as follows:

$$v_{l-i} = \frac{l_i}{\Delta t_i'} \tag{1}$$

$$l_i = i \cdot D \tag{2}$$

https://doi.org/10.1021/acsomega.4c03972
ACS Omega 2024, 9, 36421−36433

Where, l_i represents the distance to sensor PS_1; D represents the distance between adjacent sensors(200 mm); i represents the pressure sensor code (PS_{1-4}); $\Delta t'_i$ represents the time difference between adjacent peak pressure signals, as shown in Figure 6.

As can be seen from Figure 7, with the increase of detonation duration (2.0−4.0 s), the maximum peak detonation pressure YY (lignite) and TS (anthracite) of the two types of coal show an upward trend. For "YY (lignite) ", the maximum peak pressure of detonation gradually rises, indicating an increase in energy release from lignite during detonation. This may be related to the higher volatiles and lower carbon content of lignite. For "TS (anthracite) ", the maximum peak detonation pressure also showed an upward trend. Compared with "YY (lignite) ", the continuous peak detonation pressure of "TS "was always 1.4% higher than that of YY, and the growth rate was smaller than that of lignite, showing a more stable performance. In terms of RDW propagation speed, with the increase of continuous explosion duration, the basic change trend of the two types of coal is basically consistent with the change trend of the peak detonation pressure. At the same time, the RDW propagation speed of TS (anthracite) is at least 5.5% higher than that of YY (lignite), reflecting more stable and efficient fuel energy release characteristics.

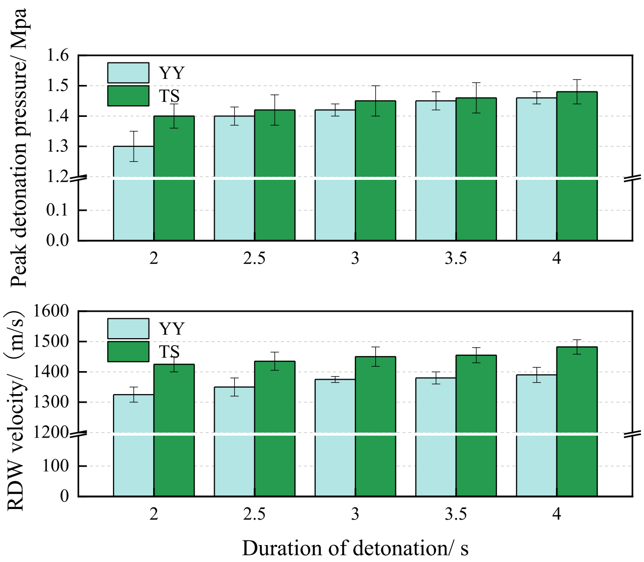

Figure 7. Propagation characteristics of two kinds of pulverized coal detonation waves.

3.2. Gas Composition Analysis. *3.2.1. Elemental Gas Analysis.* To investigate the variation of gas products during the continuous detonation of coal dust/methane, the experiment examines the changes in the content of various components in the gas products under different detonation stable state durations. After coal dust/methane detonation, the main gases are N_2, O_2, CO_2, CO, in addition to a small amount of methane (CH_4), ethane (C_2H_6), ethylene (C_2H_4), acetylene (C_2H_2), and other trace hydrocarbon gases. Therefore, the elements present in the gas products are nitrogen, oxygen, hydrogen, carbon, and trace amounts of other elements.

Figure 8 presents the residual gas compositions of $\varphi(O_2)$, $\varphi(N_2)$, and $\varphi(H_2)$ following methane/air and methane/coal dust/air detonations. From Figure 8a, it is evident that as the duration of continuous detonation increases from 0.20 s to 0.30 s, $\varphi(O_2)$ significantly reduces from 3% to 1%. Further extending the detonation duration from 0.30s to 0.40s results in a gradual decrease of $\varphi(O_2)$ from 1% to 0.3%. For 12% methane and coal dust mixture, regardless of whether TS pulverized coal or YY pulverized coal, the $\varphi(O_2)$ was almost entirely consumed. Compared to the detonation of 12% methane alone, the oxygen consumption in the detonation of a 12% methane and coal dust mixture is substantially higher, even for continuous detonations lasting only 0.2s.

From Figure 8b, it is evident that after the detonation of pure gaseous fuel with 12% methane, the concentration of nitrogen (N_2) is relatively high. Additionally, as the duration of the detonation increases, the nitrogen content remains largely unchanged. And that is because the volume fraction of a gas is relative to the volume percentage. N_2 is actually nonreactive during detonation, resulting in a condensation effect that produces a very high $\varphi(N_2)$ gas (even more than 78%) due to the consumption of other gaseous fuels. Therefore, $\varphi(N_2)$ will produce a small range of data fluctuations. However, with the addition of coal dust, $\varphi(N_2)$ decreases with the increase of coal dust concentration. This is because the volume fraction of gas products after detonation of pulverized coal and other gases increases, resulting in the decrease of $\varphi(N_2)$. However, with the addition of coal dust, $\varphi(N_2)$ decreases with the increase of coal dust concentration. This is because the volume fraction of gas products after detonation of pulverized coal and other gases increases, resulting in the decrease of $\varphi(N_2)$. Compared with 12% CH_4 mixed YY, 12% CH_4 mixed TS has a lower $\varphi(N_2)$ value, indicating that lignite produces more other gases. However, with the addition of coal dust, $\varphi(N_2)$ decreases with the increase of coal dust concentration. This is because the volume fraction of gas products after detonation of pulverized coal and other gases increases, resulting in the decrease of $\varphi(N_2)$. Compared with 12% CH_4 mixed YY pulverized coal, 12% CH_4 mixed TS pulverized coal has a lower $\varphi(N_2)$ value, indicating that lignite produces more other gases. When the continuous detonation time increases from 0.2s to 0.3s, the $\varphi(N_2)$ after detonation decreases significantly, and when the continuous detonation time exceeds 0.3s, the $\varphi(N_2)$ decreases slowly, which indicates that 0.3s belongs to a relatively stable detonation state during the continuous detonation process of pulverized coal/methane.

Figure 8c illustrates the ratio of $\varphi(H_2)$ in gases after detonation. Typically, the detonation combustion of coal dust/CH_4 does not produce H_2, as hydrogen atoms initially react with oxygen to form water vapor, and carbon is oxidized in a perfect ideal state. However, when there is a significant deficiency of O_2 to fully oxidize CH_4, thermal decomposition of CH_4 occurs, resulting in the production of H_2. For 12% CH_4 gas detonation, when the continuous detonation duration is 0.2s, the hydrogen production increases slowly, and when the continuous detonation duration is increased to 0.4s, $\varphi(H_2)$ reaches about 6%. In the pulverized coal/methane detonation process, the more sufficient the detonation combustion reaction, the less oxygen involved in the reaction, and the more hydrogen may be produced. When 12% CH_4 is added to coal dust, $\varphi(H_2)$ in the gas after detonation increases with the increase of continuous detonation time. When the continuous detonation time exceeds 0.27s, the amount of hydrogen produced by YY pulverized coal/12% CH_4 fuel is greater than that by TS pulverized coal/12% CH_4 continuous detonation. When the continuous detonation time is 0.4s, the gas $\varphi(H_2)$

https://doi.org/10.1021/acsomega.4c03972
ACS Omega 2024, 9, 36421−36433

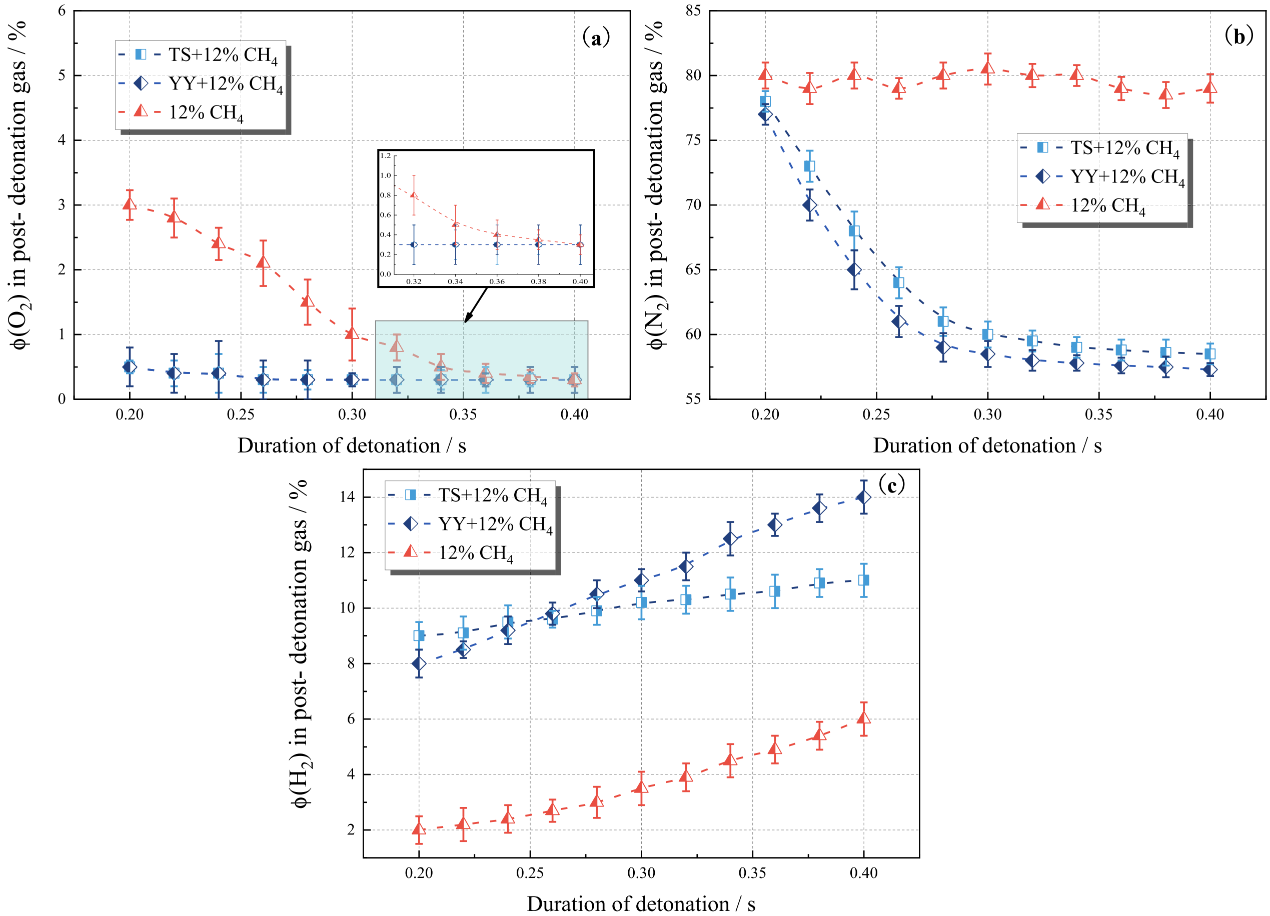

Figure 8. Volume fraction of elemental gas after detonation (a: O_2; b: N_2; c: H_2).

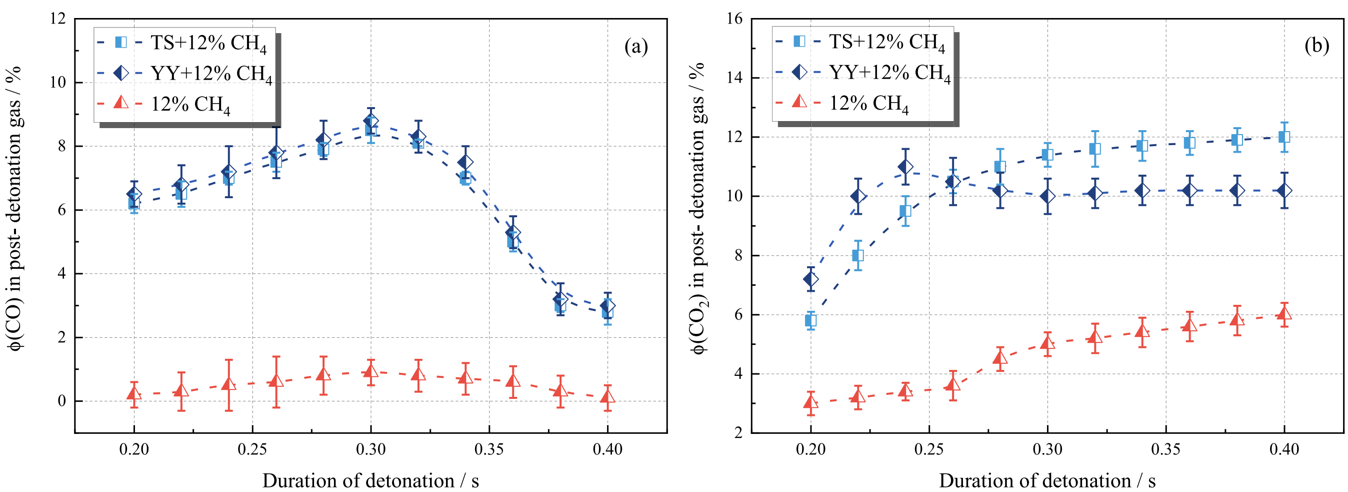

Figure 9. Volume fraction of elemental gas after detonation(a: CO; b: CO_2).

after detonation of TS pulverized coal/12% CH_4 and YY pulverized coal/12% CH_4 are 14.2% and 10.8%, respectively, which are much higher than the $\varphi(H_2)$ produced after detonation of 12% CH_4. It can be inferred that anthracite pulverized coal is a more stable fuel in the continuous detonation stage than lignite pulverized coal.

3.2.2. Compound Analysis of Gas Products. Figure 9 shows $\varphi(CO)$ and $\varphi(CO_2)$ in the postdetonation gases. In general, $\varphi(CO)$ and $\varphi(CO_2)$ in the gas produced after pulverized coal/methane detonation are higher than that produced by pure gas fuel (methane) detonation.

As can be seen from Figure 9a, when the continuous detonation time increases from 0.2 s to 0.3 s, $\varphi(CO)$ begins to increase slowly and then decreases gradually. $\varphi(CO)$ of 12% CH_4 increases from 0.2 to 0.9% after detonation and then decreases to 0.1% at 0.4 s. When mixed with pulverized coal/12% CH_4 produced more CO. Under the same detonation duration, the increase of $\varphi(CO)$ in the gas produced by YY/12% CH_4 was greater than that of TS/12% CH_4. In general, CO is produced due to incomplete combustion of pulverized coal/methane during detonation. In this study, anthracite shows more stable detonation fuel characteristics.

As can be seen from Figure 9b, the $\varphi(CO_2)$ in the gas after detonation first increases and then remains unchanged as the continuous detonation time increases. The peak $\varphi(CO_2)$ value of 12% CH_4 detonation is 6.1%. When mixed with coal dust, CH_4 detonation produces more CO_2. The peak values of $\varphi(CO_2)$ of TS and YY were 12.1% (t = 0.4 s) and 10.9% (t = 0.24 s), respectively. The volatile content of lignite is higher than that of anthracite. In the early stage of detonation, volatiles react with oxidants to release a large amount of CO_2 rapidly. As the continuous detonation time increases, the volatile content of lignite decreases and the volume fraction of non-CO_2 gaseous products increases, resulting in a decrease of $\varphi(CO_2)$. The fixed carbon content of anthracite is large and stable, and the $\varphi(CO_2)$ content increases gradually.

The ratio of $\varphi(CO)/\varphi(CO_2)$ can reflect the relative excess amount of fuel in detonation combustion reaction to a certain extent. Figure 10 shows the $\varphi(CO)/\varphi(CO_2)$ of the gas after detonation. It can be found that $\varphi(CO)/\varphi(CO_2)$ gradually decreases with the increase of continuous detonation time. In the early stage of detonation (t = 0.2 s), pulverized coal/CH_4 is more sensitive to $\varphi(CO)/\varphi(CO_2)$ than pure gas fuel CH_4.

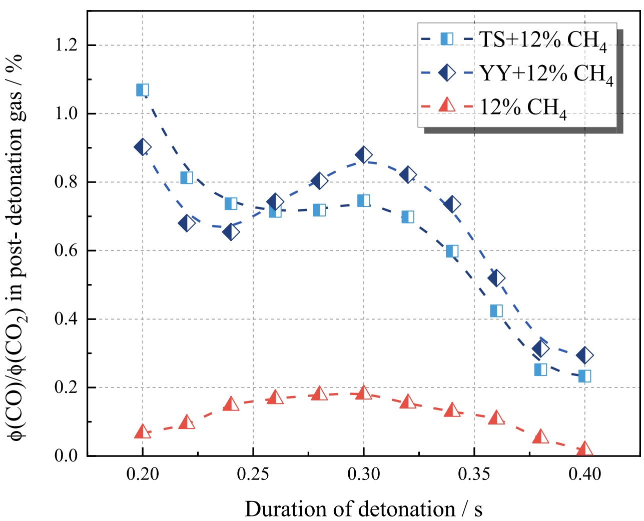

Figure 10. $\varphi(CO)/\varphi(CO_2)$ in post-detonation gases.

On the other hand, it can be seen from the above analysis results that the concentration of O_2 after pulverized coal detonation is basically less than 12%, which is far lower than the oxygen concentration of air species. In addition, the release of CO gas not less than 2000 ppm poses a challenge to human life and health, and there are hidden dangers of poisoning. Therefore, it is necessary to effectively collect the gas of pulverized coal in the RDE device, prohibit direct discharge, and strengthen the effective ventilation of the RDE device when it works, which is of great significance for the application of the RDE device in deep coal fluidization mining.

In addition to C_xO_y compound gas, C_xH_y is also a compound gas generated by pulverized coal/gas solid fuel after detonation through physicochemical reactions such as desorption, pyrolysis and intense combustion. Table 2 shows the gas composition generated after detonation of two kinds of coal. It can be seen that for hydrocarbon gases, the relative content of CH_4 is higher than that of other gases (C_2H_2, C_2H_4, C_2H_6, C_3H_8), followed by the order of gas content from high to low: C_2H_4, C_2H_2, C_2H_6, C_3H_8. From the results of hydrocarbon gas composition of the two types of coal, it can be seen that there is a slight difference in the volume fraction of hydrocarbon gas generated after detonation of lignite/methane and anthracite/methane. Although there is little difference in the volume fraction of hydrocarbon gases generated after detonation between lignite and anthracite, these differences reflect subtle differences in the chemical composition of coal, detonation conditions, and reaction paths. These findings have important implications for understanding how different types of coal perform in RDE and for optimizing fuel selection and detonation processes.

Table 2. Composition Table of Hydrocarbon Gases Generated by Detonation of Two Types of Coal

	volume fraction/(1×10^{-2})				
type of coal	CH_4	C_2H_2	C_2H_4	C_2H_6	C_3H_8
TS	0.79	0.22	0.32	0.12	0.08
YY	0.80	0.23	0.35	0.13	0.09

3.3. Flammability Analysis of Gas Products. The gas generated by detonation contains a variety of components, and if it has certain flammability, it will inhibit the continuous detonation and disturb the normal detonation work. The flammability analysis of detonation tail gas can be calculated as follows:

$$A_i' = \frac{A_i}{\sum_{i=1}^{N} A_i + \sum_{k=1}^{P} K_k B_k} \quad (3)$$

$$R = \sum_{i=1}^{N} 100 \times \frac{A_i'}{T_{Ci}} \quad (4)$$

Where, A_i' represents the equivalent amount of flammable gas; A_i is the molar fraction of the i_{th} flammable gas in the mixture, %; K_k represents the equivalent factor of an inert gas relative to nitrogen; B_k represents the molar fraction of the k_{th} inert gas in the mixture,%. K_k (N_2) = 1, and $K_k(CO_2)$ = 1.5; T_{Ci} represents the highest content of flammable gas when it is not flammable in the air after mixing with nitrogen. $T_{Ci}(CO)$ =15.2, and $T_{Ci}(H_2)$=15.2. R is the flammability value of the gas mixture. The evaluation of the flammability R value of the mixed gas is shown in eq 5:

$$\begin{cases} R > 1; & \text{Flammable} \\ R \le 1; & \text{Not flammable} \end{cases} \quad (5)$$

After a gas (coal dust) detonation, the gas may contain a non-negligible amount of oxygen. In cases where multiple flammable gases, various inert gases, and significant oxygen coexist, they need to be simplified into a mixture of multiple flammable gases, one inert gas, and oxygen for flammability calculations. Since the volume fraction of nitrogen is much higher than that of carbon dioxide, inert gases are approximated as nitrogen to reduce calculation errors. Under these conditions, the flammability of the mixture gas must satisfy the conditions of eq 6:

$$\begin{cases} \sum X_i \ge T_{Ci,F} \\ \sum X_i \ge L_m \end{cases} \quad (6)$$

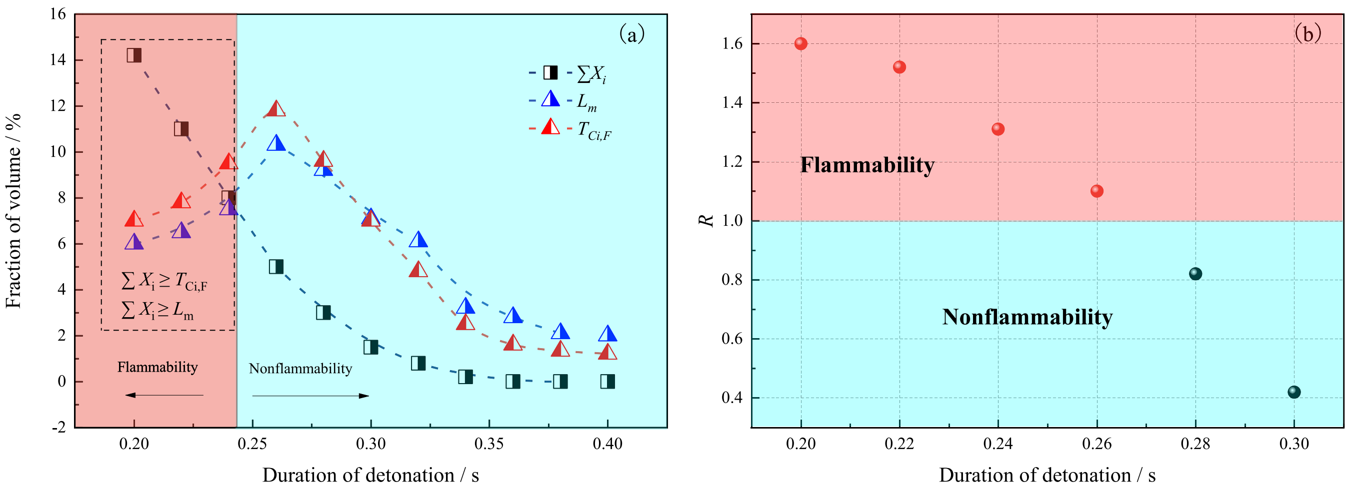

Figure 11. Evaluation of the combustibility of the detonation generated gas of YY coal (a, parameter relation; b, flammability evaluation results).

$$T_{Ci,F} = \frac{\sum A_i}{\sum (A_i/T_{Ci})} \times (1 - 4.76x_0) \quad (7)$$

$$L_m = \frac{\sum A_i}{\sum (A_i/L_{i(L)})} \quad (8)$$

Where, $\sum X_i$ represents the volume fraction of the flammable gas in the mixture, %;$L_{i(L)}$ is the lower flammability limit of a flammable gas, %; x_0 is the volume fraction of oxygen in the gas mixture, %

The gas product of pulverized coal/gas gas−solid fuel mixture produced by detonation combustion still has certain flammability properties. As can be seen from Figure 11, Within the detonation duration of 0.2 s to 0.26 s, the gas generated by the detonation of YY coal/gas solid fuel is combustible. When the detonation duration exceeds 0.26 s, the gas generated by detonation has no flammability. Figure 12 compares the changing law of the combustibility of the gas generated by detonation of TS coal and TA coal. It can be seen that the combustibility of the gas generated by detonation of lignite is more sensitive to the detonation duration than that of anthracite coal. During the experimental process, secondary ignition of gases produced by detonation affects the coupling reaction of continuous detonation, causing the continuous detonation wave to decouple. Consequently, anthracite solid fuel exhibits a certain stability, which constitutes a fundamental difference from the results of deflagration combustion gases.[36]

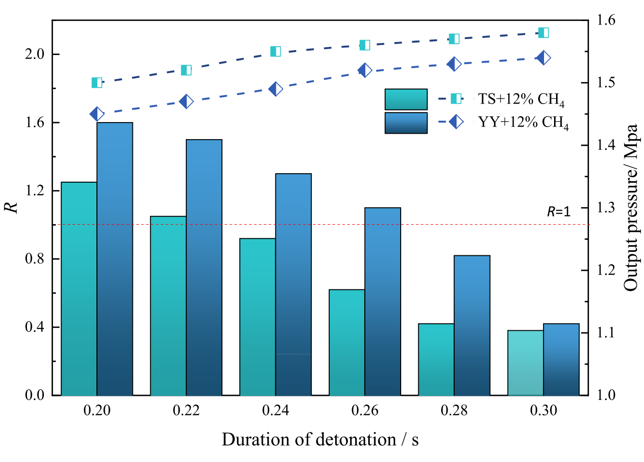

Figure 12. Comparison of combustibility and fuel properties of two kinds of coal.

3.4. The Gaseous Product Trends. Based on the results of pulverized coal detonation gas release and the combustion mechanism of typical pulverized coal, this section studies the different stages of pulverized coal detonation gas release and the change of trend.

Figure 13 shows the three stages and evolution rules of pulverized coal detonation gas products. According to the ZND model, a detonation wave consists of a shock wavefront (von Neumann spike), an induction zone, and a reaction zone. During coal dust detonation, these three regions correspond to different reaction stages and gas product evolution patterns: at the shock wavefront (i.e., the initial stage of detonation), the coal dust undergoes intense shock compression and heating, causing a rapid increase in temperature and pressure, which initiates the pyrolysis of organic components in the coal dust. This stage primarily generates small molecular products such as methane (CH_4), water vapor (H_2O), and solid carbon (C), providing combustible substances for subsequent oxidation reactions. In the induction zone (i.e., the second stage), the pyrolysis products undergo intense gas−solid coupled reactions with oxygen (O_2) in the air. CH_4 and other combustible gases (C_xH_y) react with O_2 at high temperatures, producing CO_2, CO, and other products while releasing a large amount of heat, further increasing the temperature. Simultaneously, dehydration and deoxygenation reactions occur on the surface of coal dust particles, accelerating the transformation of coal dust into final products. In the reaction zone (i.e., the third stage), as the temperature continues to rise, gas-phase reactions intensify, generating more CO_2. However, due to the consumption of oxygen, gas-phase reactions gradually weaken, and the unburned carbon reacts with CO_2 at high temperatures to produce CO. Additionally, under oxygen-deficient conditions, CH_4 undergoes thermal cracking, producing H_2 and C. The reactions in this stage are the most intense, and the product composition tends to stabilize. In summary, the ZND model effectively explains the evolution patterns and kinetic characteristics of gaseous products during coal dust detonation. The changes in reaction mechanisms and product composition at different stages are closely related to the three regions in the ZND model.

https://doi.org/10.1021/acsomega.4c03972
ACS Omega 2024, 9, 36421−36433

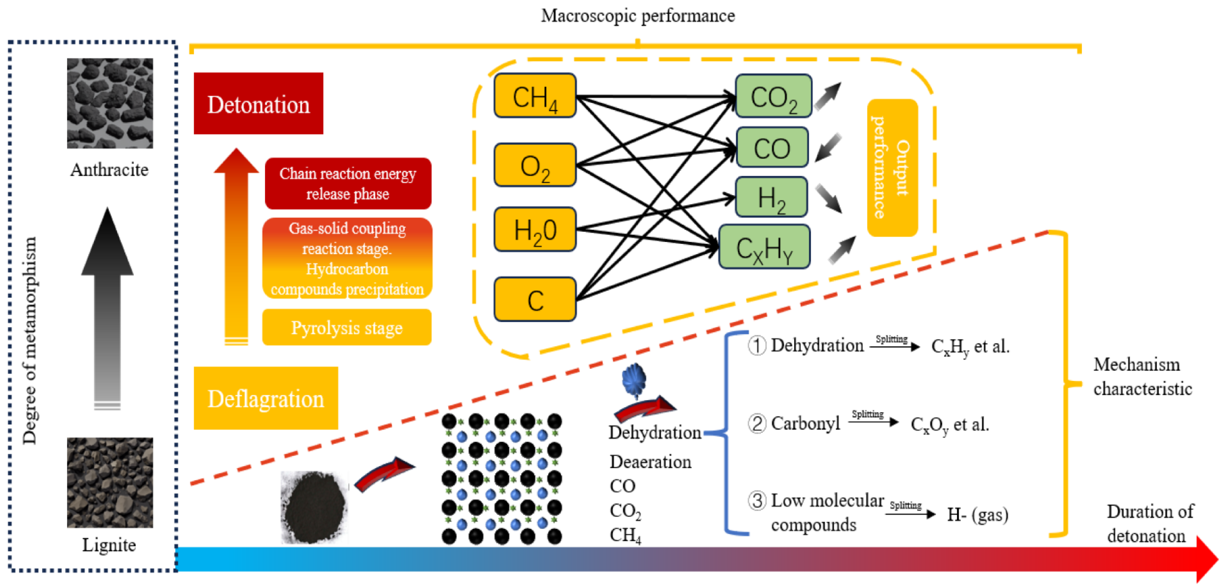

Figure 13. Three stages and evolution law of pulverized coal detonation gas products.

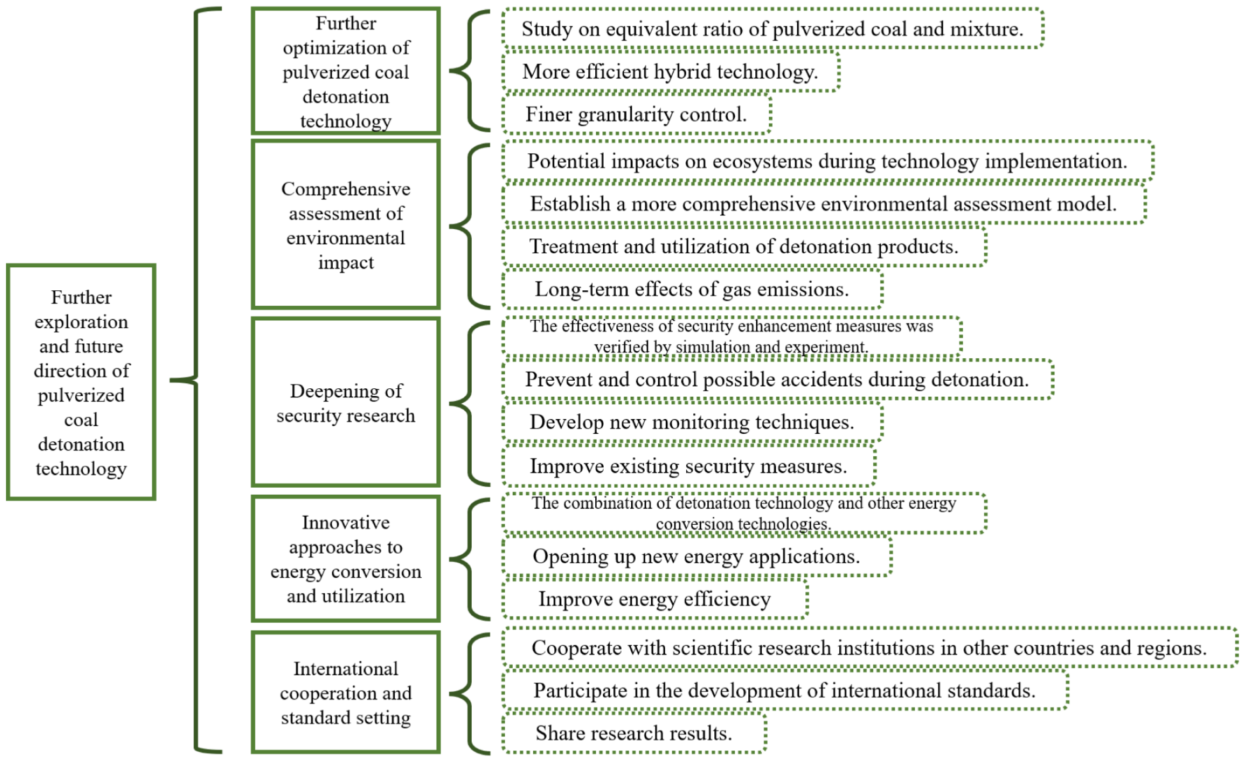

Figure 14. A technical framework for in-depth exploration and future directions of pulverized coal detonation.

In terms of the advantages of pulverized coal fuel, due to the chemical composition, the fixed carbon content (FC_{ad}) of anthracite (TS) is 82.54%, while that of lignite (YY) is only 47.6%. This indicates that anthracite has a higher fixed carbon content, which is generally associated with more stable combustion characteristics and a higher calorific value. In addition, the volatile content (Vad) of lignite is 37.5%, which is much higher than the 8.1% of anthracite. This means that when lignite is heated, it quickly releases a large amount of volatile gases, which can promote the rapid propagation of detonation waves, but at the same time can also cause combustion instability. In the detonation process, when 12% methane is mixed with coal dust for detonation, whether it is TS coal dust or YY coal dust, the oxygen consumption ($\varphi(O_2)$) is almost completely consumed. This indicates that both coal fuels can effectively participate in the reaction and promote the release of energy during detonation. However, from the $\varphi(N_2)$ data, the TS coal dust mixed with 12% methane has a lower nitrogen content after detonation, suggesting that anthracite may have produced more other gases during detonation, which may be related to its higher fixed carbon content, which provides more heat and propulsion. In addition, from the perspective of $\varphi(H_2)$, the hydrogen yield of anthracite (TS) during detonation is higher

https://doi.org/10.1021/acsomega.4c03972
ACS Omega 2024, 9, 36421−36433

than that of lignite (YY), which may be due to the more complete combustion reaction of anthracite during detonation. This is also reflected in the data of $\varphi(CO)$ and $\varphi(CO_2)$. The CO_2 production of anthracite is higher than that of lignite, while the CO production is relatively low, indicating that anthracite is burned more completely. On the whole, although lignite may have some advantages in the early stage of detonation due to the rapid release of volatile compounds, anthracite (TS) shows more superior fuel characteristics in terms of overall detonation stability, combustion completeness and environmental impact. The high fixed carbon content and low volatile matter of anthracite make it able to provide more stable energy output and higher combustion efficiency in the detonation process, which is very important for the pursuit of high efficiency and environmental friendly detonation process in practical applications.

4. DISCUSSION

Based on the research results of this paper, this section focuses on the prospect of the engineering application of pulverized coal/gas detonation energy efficient release technology, especially in the aspect of energy efficient utilization and safe operation, which is crucial for the design of more efficient and environmentally friendly pulverized coal detonation system.

The use of coal dust detonation technology is increasingly prevalent in the field of energy science, particularly within rotating detonation engines (RDE) where coal and methane (CH_4) are employed as fuels. The focus of research has shifted toward the pressure characteristics and the secondary detonation effects of the gases produced. The further optimization and application of coal powder detonation technology still face multiple challenges, necessitating the development of scientific and technical strategies. The technical framework for exploring pulverized coal detonation in depth is shown in Figure 14. First, the technology requires further refinement, particularly in controlling particle size and improving mixing techniques. Efficient mixing ensures thorough contact between coal powder and oxidizers, enhancing reaction efficiency. Current research is exploring unconventional methods such as ultrasonics and electromagnetic fields to achieve more uniform mixing. In Rotating Detonation Engines (RDE), the mixture of coal powder and methane generates high-pressure gases during detonation, crucial for engine performance and efficiency. Studies indicate that lignite and anthracite exhibit different detonation characteristics when mixed with methane, due to their inherent chemical and physical properties. This variance is significant for the design and operation of RDEs, as different coal types may require tailored operational parameters to optimize performance.

Additionally, the secondary detonation effect of the generated gases is a key issue in RDE technology. In the high-temperature, high-pressure conditions of RDE detonation, unburned mixtures of coal powder and methane may reignite upon cooling, affecting engine stability and potentially causing safety incidents. Therefore, controlling this process is vital for enhancing RDE safety and efficiency. Research has shown that adjusting fuel ratios and ignition parameters can effectively control the likelihood and intensity of secondary detonations. Environmental impact assessments are crucial for the sustainable development of this technology. Comprehensive evaluations of gas emissions, solid waste management, and potential ecological impacts are needed. For instance, harmful gases like NOx and SOx produced during coal powder detonation must be treated with advanced purification technologies to meet increasingly stringent environmental standards. Additionally, strategies for resource utilization of postdetonation solid residues, such as converting them into building materials or soil amendments, are essential. Safety research is fundamental to ensuring the application of coal powder detonation technology. With technological advancements, new monitoring and control systems are being developed to oversee the detonation process and prevent potential accidents. For example, using high-speed cameras and pressure sensors to monitor the propagation of detonation waves allows for timely detection of anomalies and corrective actions. Furthermore, extensive simulations and experimental validations systematically assess various safety aspects. In terms of energy conversion pathways, coal powder detonation technology not only serves traditional power generation but also holds potential for applications in synthetic gas production and hydrogen generation. Adjusting detonation parameters can optimize the yield and ratio of syngas (mainly carbon monoxide and hydrogen), which is crucial for synthetic fuel and chemical production. Additionally, the application of this technology in hydrogen production demonstrates high efficiency and lower carbon emissions, contributing to the advancement of clean energy. International collaboration plays a vital role in advancing coal powder detonation technology. By sharing research outcomes and accelerating technological innovation and standardization, multinational research institutions and enterprises have established cooperative networks. The future development of coal powder detonation technology should focus on technological optimization, environmental impact assessment, safety enhancement, and exploring new energy conversion pathways. These comprehensive measures will effectively promote the widespread application and continuous development of the technology, making significant contributions to global energy transformation and environmental protection.

5. CONCLUSIONS

This study investigated the detonation characteristics and gas product ejection properties of brown coal and anthracite dust mixed with methane in a rotating detonation engine (RDE). The findings provide valuable insights into the combustion behavior and gas product composition of different coal types, which is crucial for optimizing coal dust detonation systems to enhance energy efficiency and reduce environmental impact. The specific findings are as follows:

(1) Using pressure sensors in the RDE, it was observed that anthracite exhibited a maximum explosion pressure peak 1.4% higher than brown coal, with a slower growth rate, indicating more stable performance. Moreover, the propagation velocity of the rotating detonation wave (RDW) in anthracite was at least 5.5% faster than in brown coal, reflecting anthracite's stability and efficiency in fuel energy release.

(2) As the detonation duration increased, both anthracite and brown coal showed nearly complete consumption of oxygen ($\varphi(O_2)$) and a significant decrease in the proportion of nitrogen ($\varphi(N_2)$) after the explosion. In terms of flammability, the brown coal/methane mixture exhibited transient flammability during the initial stage of the explosion, while anthracite displayed more persistent flammability.

(3) Although brown coal may have some advantages in the early stages of the explosion due to the rapid release of

https://doi.org/10.1021/acsomega.4c03972
ACS Omega 2024, 9, 36421−36433

volatiles, anthracite demonstrated superior fuel characteristics throughout the entire detonation process, including more stable combustion properties, higher energy output, and lower environmental impact. The results of this study emphasize the importance of pursuing efficient and environmentally friendly detonation processes in practical applications and highlight the need for future research to further explore technological optimizations, environmental impact assessments, and safety enhancement measures.

AUTHOR INFORMATION

Corresponding Author

Jing Guo − *China University of Mining and Technology - Beijing, Beijing 100083, China;* orcid.org/0000-0003-1642-4054; Email: yizeown@163.com

Authors

Shirong Ge − *China University of Mining and Technology - Beijing, Beijing 100083, China*
Ruibo Yang − *China University of Mining and Technology - Beijing, Beijing 100083, China*
Jiayu Liang − *China University of Mining and Technology - Beijing, Beijing 100083, China*
Yinan Guo − *China University of Mining and Technology - Beijing, Beijing 100083, China*

Complete contact information is available at: https://pubs.acs.org/10.1021/acsomega.4c03972

Author Contributions

J.G. and S.G. contributed to conceptualization; J.G. contributed to methodology; J.G. contributed to software; S.G., Y.G. and R.Y. contributed to validation; J.G. contributed to formal analysis; J.G. contributed to investigation; S.G. contributed to resources; J.G. contributed to data curation; writing—original draft preparation, J.G. contributed to data curation; J.G. contributed to writing—review and editing; J.G. contributed to visualization; J.G. contributed to supervision; J.G. contributed to project administration; S.G. contributed to funding acquisition. All authors have read and agreed to the published version of the manuscript.

Funding

This research was funded by the Natural Science Foundation of China (Major Program), grant number 52121003.

Notes

The authors declare no competing financial interest.

REFERENCES

(1) Xi, X.; Teng, H.; Chen, Z.; Yang, P. Effects of longitudinal disturbances on two-dimensional detonation waves. *Phys. Rev. Fluids* **2022**, *7*, 043201.
(2) Crane, J.; Lipkowicz, J. T.; Shi, X.; Wlokas, I.; Kempf, A. M.; Wang, H. Three-dimensional detonation structure and its response to confinement. *Proc. Combust. Inst.* **2023**, *39*, 2915−2923.
(3) Pan, Z.; Jiang, N.; Zhou, J.; Zhang, P. Dynamic behavior of detonation waves in millimeter-scale tubes: unraveling the influence of tube diameter, initial pressure, and mixture. *Exp. Fluids* **2024**, *65*, 13.
(4) Liu, D.-Y.; Zhao, P.; Chan, S. H.-Y.; Hng, H. H.; Chen, L. Effects of nano-sized aluminum on detonation characteristics and metal acceleration for RDX-based aluminized explosive. *Def. Technol.* **2021**, *17*, 327−337.
(5) Bykovskii, F. A.; Zhdan, S. A.; Vedernikov, E. F. Parameters of Continuous Multifront Detonation of a Methane Mixture with Heated Air in an Annular Cylindrical Combustor. *Combust., Explos. Shock Waves* **2022**, *58*, 149−158.
(6) Wang, L. Q.; Ma, H. H. Detonation propagation limits in hydrogen-oxygen mixtures in a tube filled with repeated perforated plates. *Int. J. Hydrogen Energy* **2022**, *47*, 645−650.
(7) Sun, X. X.; Lu, S. X. Effect of orifice shapes on the detonation transmission in $2H_2$-O_2 mixture. *Int. J. Hydrogen Energy* **2020**, *45*, 2360−2367.
(8) Meng, H. L.; Xiao, Q.; Feng, W. K.; Wu, M. L.; Han, X. P.; Wang, F.; Weng, C. S.; Zheng, Q. Air-breathing rotating detonation fueled by liquid kerosene in cavity-based annular combustor. *Aerosp. Sci. Technol.* **2022**, *122*, 107407.
(9) Xie, H.; Ju, Y.; Ren, S.; Gao, F.; Liu, J.; Zhu, Y. Theoretical and technological exploration of deep in situ fluidized coal mining. *Front. Energy* **2019**, *13*, 603−611.
(10) Ju, Y.; Nie, X.; Zhu, Y.; Xie, H. In situ fluidized mining and conversion solution to alleviate geological damage and greenhouse gasemissions due to coal exploitation: A numerical analysis and evaluation. *Energy Sci. Eng.* **2021**, *9* (1), 40−57.
(11) Xie, H.; Ju, Y.; Gao, F.; Gao, M.; Zhang, R. Groundbreaking theoretical and technical conceptualization of fluidized mining of deep underground solid mineral resources. *Tunn. Undergr. Space Technol.* **2017**, *67*, 68−70.
(12) Ju, Y.; Zhu, Y.; Xie, H.; Nie, X.; Zhang, Y.; Lu, C.; Gao, F. Fluidized mining and in-situ transformation of deep underground coal resources: a novel approach to ensuring safe, environmentally friendly, low-carbon, and clean utilisation. *Int. J. Coal Sci. Technol.* **2019**, *6*, 184−196.
(13) Ranjith, P. G.; Zhao, J.; Ju, M.; De Silva, R. V.; Rathnaweera, T. D.; Bandara, A. K. Opportunities and challenges in deep mining: a brief review. *Engineering* **2017**, *3* (4), 546−551.
(14) Voitsekhovskii, B. V. Statsionarnaya dyetonatsiya. *Doklady Akademii Nauk SSSR* **1959**, *129* (6), 1254−1256.
(15) Frolov, S. M.; Zvegintsev, V. I.; Ivanov, V. S.; et al. Wind tunnel tests of a hydrogen-fueled detonation ramjet model at approach air stream Mach numbers from 4 to 8. *Int. J. Hydrogen Energy* **2017**, *42* (40), 25401−25413.
(16) Frolov, S. M.; Zvegintsev, V. I.; Ivanov, V. S.; et al. Hydrogen-fueled detonation ramjet model: Wind tunnel tests at approach air stream Mach number 5.7 and stagnation temperature 1500 K. *Int. J. Hydrogen Energy* **2018**, *43* (15), 7515−7524.
(17) Smith, R. D.; Stanley, S. B. Experimental investigation of rotating detonation rocket engines for space propulsion. *J. Propulsion Power* **2021**, *37* (3), 463−473.
(18) Klapötke, T. M.; Suceska, M. A Computational Study on the Detonation Velocity of Mixtures of Solid Explosives with Non-Explosive Liquids. *Propellants, Explos., Pyrotech.* **2021**, *46* (3), 352−354.
(19) Gimaltdinov, I. K.; Lepikhin, S. A. On Counteracting a Detonation Wave in a Bubbly Liquid Using Small-Amplitude Waves. *High-Temp.* **2023**, *61* (6), 818−823.
(20) Ren, J. F.; Bai, C. H.; Chang, C. Y.; Peng, X.; Li, B.; Jing, Q. Experimental and numerical simulation study on the dispersion and explosion process of solid-liquid-air mixed three phase components. *Combust. Flame* **2024**, *261*, 113336.
(21) Wang, X. W.; Wang, Z. R.; Ni, L.; Zhu, M.; Liu, C. P. Explosion characteristics of aluminum powder in different mixed gas environments. *Powder Technol.* **2020**, *369*, 53−71.
(22) Garan, N.; Dybe, S.; Paschereit, C. O.; Djordjevic, N. Consistent emission correction factors applicable to novel energy carriers and conversion concepts. *Fuel* **2023**, *341*, 127658.
(23) Hou, Z. H.; Wang, D. M.; Zhang, W.; Luo, S. Y.; Lu, Y. S.; Tian, S. Y.; Zhong, Q.; Xu, Z. M. Study on the influence of ignition position on the explosion characteristics of methane-air premix in a semi-closed pipeline. *Process Saf. Environ. Prot.* **2023**, *172*, 642−651.
(24) Liang, Y. T.; Lei, B. W.; Song, S. L.; Xiao, J. J.; Kuznetsov, M.; Jordan, T. Numerical analysis of the distribution of combustion products from methane explosions in a full-scale tunnel using all-speed CFD code GASFLOW-MPI. *Energy Sources, Part A* **2023**, *45*, 7105−7121.

(25) Xu, D.; Mu, C.; Li, Z.; Zhang, W. Influence of Cavi Width on Attenuation Characteristic of Gas Explosion Wave. *S Noise Control.* **2021**, *2021*, 6634754.
(26) Bykovskii, F. A.; Vedernikov, E. F.; Zholobov, Y. A. Detonation combustion of lignite with titanium dioxide and water additives in air. *Combust Explos Shock Waves* **2017**, *53*, 453−460.
(27) Bykovskii, F. A.; Zhdan, S. A.; Vedernikov, E. F.; et al. Detonation burning of anthracite and lignite particles in a flow-type radial combustor. *Combust. Explos. Shock Waves* **2016**, *52*, 703−712.
(28) Bykovskii, F. A.; Zhdan, S. A.; Vedernikov, E. F.; et al. Detonation of a coal-air mixture with addition of hydrogen in plane-radial vortex chambers. *Combust. Explos. Shock Waves* **2011**, *47*, 473−482.
(29) Bykovskii, F. A.; Zhdan, S. A.; Vedernikov, E. F. Detonation combustion of coal. *Combust. Explos. Shock Waves* **2012**, *48*, 203−208.
(30) BykovskiĬ, F. A.; Zhdan, S. A.; Vedernikov, E. F. Continuous and pulsed detonation of a coal-air mixture. *Dokl. Phys.* **2010**, *55*, 142−144.
(31) Jia, Y.; Zhang, Q. Minimum ignition temperature of gas−liquid two-phase cloud. *J. Therm. Anal. Calorim.* **2024**, *149* (9), 3819−3831.
(32) Yang, A. B.; Liu, Y. J.; Gao, K.; Li, R.; Li, Q.; Li, S. Numerical Simulation of Gas Explosion with Non-uniform Concentration Distribution by Using OpenFOAM. *ACS Omega* **2023**, *8* (51), 48798−48812.
(33) Cveticanin, D.; Herisanu, N.; Biro, I.; Zukovic, M.; Cveticanin, L. Vibration of the Biomass Boiler Tube Excited with Impact of the Cleaning Device. *Mathematics* **2020**, *8*, 1519.
(34) Guo, J.; Ge, S.; Guo, Y.; Liang, J.; Yang, R. Study on detonation characteristics of pulverized coal and evolution law of detonation residue. *Sci. Rep.* **2024**, *14* (1), 11691.
(35) Lin, S.; Liu, Z.; Qian, J.; Li, X.; Zhang, Q. Flammability and Explosion Risk of Post-explosion CH4/air and CH4/coal dust/air Mixtures. *Combust. Sci. Technol.* **2021**, *193* (8), 1279−1292.

https://doi.org/10.1021/acsomega.4c03972
ACS Omega 2024, 9, 36421−36433